

DISCLAIMER

SRC Technical Notes are informal memos intended for internal communication and documentation of work in progress. These notes are not necessarily definitive and have not undergone a pre-publication review. If you rely on this note for purposes other than its intended use, you assume all risk associated with such use.

University of Wisconsin-Synchrotron Radiation Center TECHNICAL NOTE	<u>File No.</u> SRC-226	<u>Page</u> 1 of 15
<u>Subject:</u> Modeling of a passive fourth harmonic cavity for the Hefei Light Source upgrade HLSII	<u>Author(s):</u> R. A. Bosch	
	<u>Date:</u> February 1, 2010	

The use of a fourth-harmonic cavity is studied for the planned upgrade of the 800-MeV Hefei Light Source HLSII. Analytic modeling and simulations indicate that such a cavity can successfully suppress parasitic coupled bunch instabilities and lengthen the bunch by a factor of 2.6. For optimally lengthened bunches, the microwave instability is not expected for broadband impedances of 2 ohms or less. The modeling suggests that a fourth-harmonic cavity may be successfully used at HLSII.

1. Introduction

An upgrade of the Hefei 800-MeV ring will increase the space available for insertion devices and increase the maximum beam current to 500 mA. An 816-MHz passive fourth-harmonic cavity may be used to lengthen the bunch, thereby suppressing parasitic longitudinal coupled bunch instabilities and the microwave instability while increasing the Touschek lifetime. We describe analytic modeling and simulations for harmonic-cavity operation. The methods and notation are described in Refs. [1] and [2].

2. HLSII modeling

Before studying the effect of a harmonic cavity upon parasitic longitudinal coupled bunch instabilities and the microwave instability, we use analytic modeling and simulations to examine the coupled dipole and quadrupole Robinson instabilities that may be excited by tuning in the harmonic cavity [1]. These instabilities may prevent “optimal bunch lengthening,” where a long bunch is confined in a in an effective potential whose linear synchrotron frequency is zero.

In the 204-MHz rf system, the natural bunch length without a harmonic cavity is calculated to be 49.5 ps for the HLSII parameters shown in Table I. Using the harmonic cavity to achieve optimal lengthening is calculated to give a bunchlength of 129 ps for ring currents of 100–500 mA. The bunch is lengthened by a factor of 2.6, provided that optimal bunch lengthening is stable.

In fig. 1(a), we show analytic Robinson-instability predictions for when all rf buckets are full. For a tuning angle of -89.75° , a coupled bunch instability is excited by the harmonic cavity. When tuning in the harmonic cavity for ring currents below 100 mA, the coupled-dipole Robinson instability is predicted to occur before optimal bunch lengthening is achieved. The coupled-quadrupole instability is predicted when bunches are over lengthened for tuning angles exceeding $\sim -83^\circ$

The analytic code also predicts a fast mode-coupling Robinson instability for optimally lengthened bunches with ring currents of 100–400 mA, because the attempted solution for the coupled dipole and quadrupole frequencies and damping/growth rates does not converge. In previous studies, this non-convergence occurred when the coupled-dipole and coupled-quadrupole frequencies were nearly equal, consistent with the observed mode-coupling instability. However, the analytic code does not determine any properties of such a mode-coupling instability, including the possibility that it is Landau-damped by the nonquadratic potential well. In the case of HLSII, this mode-coupling prediction occurs when the coupled-dipole and coupled-quadrupole frequencies are very different, suggesting that the code’s mode-coupling instability prediction may be incorrect, or it may describe a mode that is Landau-damped.

Figure 1(b) shows simulation results when 100 macroparticles/bucket are simulated for 500,000 turns. If a macroparticle’s displacement from the synchronous phase exceeds one-half of the rf period, it is considered lost, in which case it is no longer tracked and its contribution to the wake is no longer computed. If any macroparticles are lost in a simulation, a solid square is plotted. Circles that indicate instability are plotted when the energy spread at the end of a simulation exceeds the natural value by more than 10%. The simulations confirm the analytic instability predictions, except for the prediction of a fast mode-coupling instability for optimally lengthened bunches. According to the simulations, stable optimally lengthened bunches are obtained for ring currents of 133-500 mA.

In fig. 2(a), analytic predictions include the possibility of parasitic coupled bunch instability caused by a typical damped HOM. Because of their broadened frequency response, damped HOMs are a frequent cause of parasitic coupled bunch instability. The predictions consider a worst-case scenario, in which the resonant frequency of the damped HOM is an integral multiple of the revolution frequency. We consider an HOM resonant frequency that equals 220 times the revolution frequency, with impedance of 10 k Ω

and quality factor of 3000. The predictions of parasitic coupled bunch instability are in approximate agreement with the simulations shown in fig. 2(b), showing that the parasitic coupled bunch instability is suppressed when the harmonic cavity is tuned for optimal bunch lengthening.

In figures 3–11, the excitation of the microwave instability by broadband impedance is considered. The broadband impedance is modeled by a HOM with resonant angular frequency $\omega_3 = c/b = 1 \times 10^{10}$ rad/s. Here, c is the speed of light and $b = 30$ mm is the radius of a round vacuum chamber that approximates the HLSII vacuum chamber's 20-mm half height and 40-mm half width. The quality factor Q_3 is one, while for $|Z_p / p| = 1 \Omega$ the resonant impedance is $R_3 = 351.1 \Omega$. Broadband impedances with $0.125 \Omega \leq |Z_p / p| \leq 32 \Omega$ are modeled in figures 3-11; each figure considers an impedance twice as large as the previous figure.

In figures 3-11, analytic predictions of microwave instability are given by the Boussard criterion [2, 3]. Simulations of 4000 macroparticles/bucket were performed by the University of Wisconsin-Madison's CONDOR® pool for high-throughput computing [4]. Each figure summarizes the results of 300 simulations that were performed simultaneously in about one day. The simulations are in rough agreement with the Boussard criterion. In previous studies, the simulations predict the microwave instability much better than the Boussard criterion, in agreement with experiments [2].

In the simulations, optimally lengthened bunches with currents up to 500 mA do not suffer from the microwave instability for $|Z_p / p| \leq 2 \Omega$.

3. Summary

Analytic modeling and simulations suggest that a fourth harmonic cavity at HLSII may be used to lengthen the bunch by a factor of 2.6 while suppressing parasitic coupled bunch instabilities from damped HOMs. For broadband impedance with $|Z_p / p| \leq 2 \Omega$, optimally lengthened bunches do not suffer from the microwave instability.

[1] R. A. Bosch, K. J. Kleman and J. J. Bisognano, Phys. Rev. ST Accel. Beams **4**, 074401 (2001).

[2] R. A. Bosch, Phys. Rev. ST Accel. Beams **8**, 084401 (2005).

[3] D. Boussard, CERN Laboratory Report No. LabII-rf-Int.-75-2, 1975.

[4] Condor Team, University of Wisconsin-Madison, *Condor Version 7.0.4 Manual* (Computer Sciences Department, University of Wisconsin-Madison, Madison, WI, 2008).

Parameter	Symbol	Value
Ring energy	E	800 MeV
Natural relative energy spread	σ_E/E	4.7×10^{-4}
Synchronous voltage	V_s	16.73 kV
Recirculation period	T_0	2.206×10^{-7} s
Fundamental rf angular frequency	ω_g	1.2817×10^9 rad/s
Number of bunches	M	45 bunches
Fundamental cavity shunt impedance	R_1^0 (unloaded)	3.3 M Ω
Fundamental cavity quality factor	Q_1^0 (unloaded)	28000
Fundamental cavity coupling coefficient	β_1	2
Harmonic-cavity harmonic number	ν	4
Harmonic-cavity shunt impedance	R_2^0 (unloaded)	2.5 M Ω
Harmonic-cavity quality factor	Q_2^0 (unloaded)	18000
Harmonic-cavity coupling coefficient	β_2	0
HOM resonant angular frequency	ω_3	6.266095955×10^9 rad/s
HOM resonant impedance	R_3	10 k Ω
HOM quality factor	Q_3	3000
Fundamental cavity maximum voltage	V_{T1}	250 kV
Momentum compaction	α	0.02
Radiation-damping time constant	τ_L	10 ms
Fundamental cavity load angle	θ_{v1}	0°

Table I. Parameters for parasitic longitudinal coupled bunch instability at HLSII (courtesy of Congfeng Wu and Lin Wang).

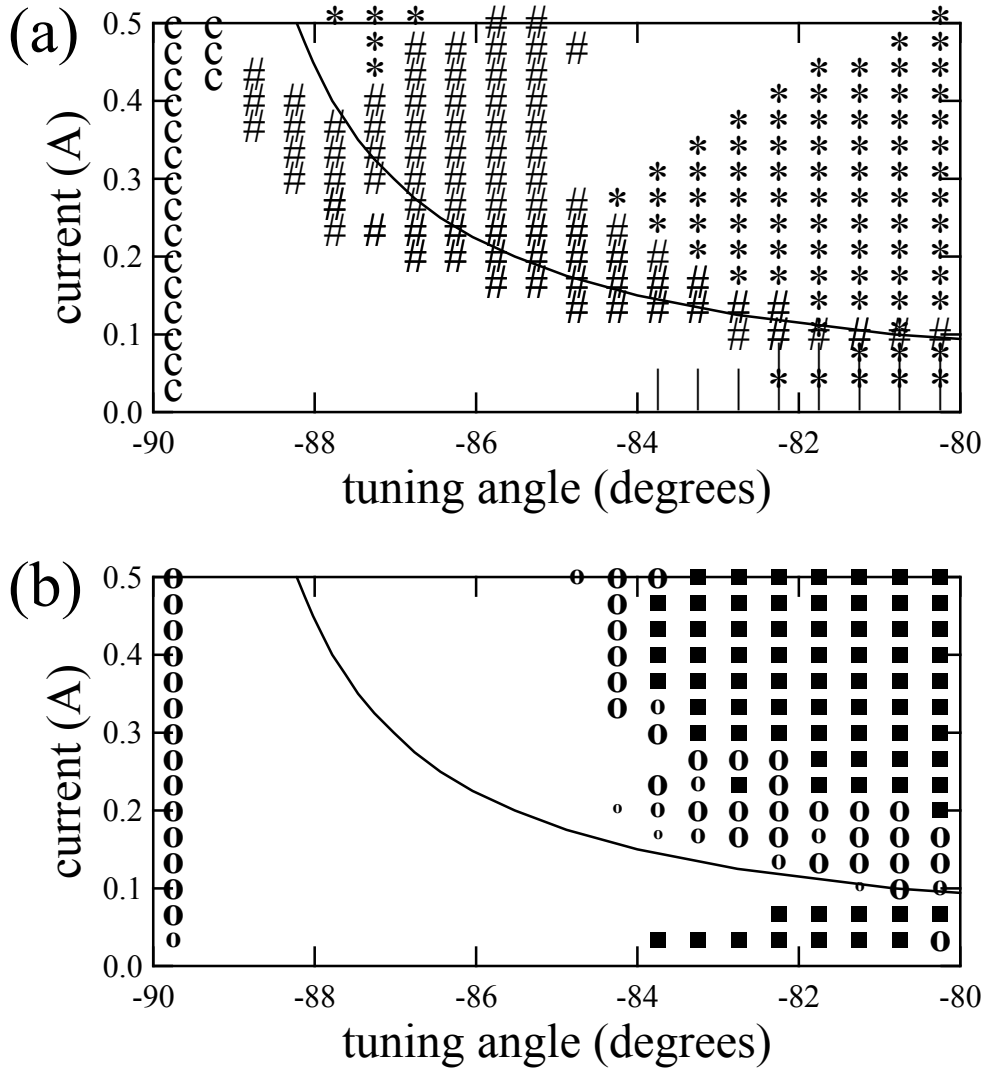


Figure 1. Instability modeling for passive harmonic-cavity operation at HLSII. A solid curve shows the parameters for optimal bunch lengthening. To the left of this curve, the bunches are “understretched” with an approximately Gaussian profile. To the right, the bunches are “overstretched” double-hump bunches. (a) Analytic instability predictions. |: coupled dipole Robinson instability; *: coupled quadrupole Robinson instability; #: fast mode-coupling Robinson instability; c: coupled-bunch instability with longitudinal mode number of 1. (b) Results of 500,000-turn simulations of 4500 macroparticles. o: mild instability, where the energy spread exceeds its natural value by 10–30%; o: moderate instability, where the energy spread has increased by 30–100%; o: strong instability, where the energy spread has increased more than 100%; ■: lost macroparticles.

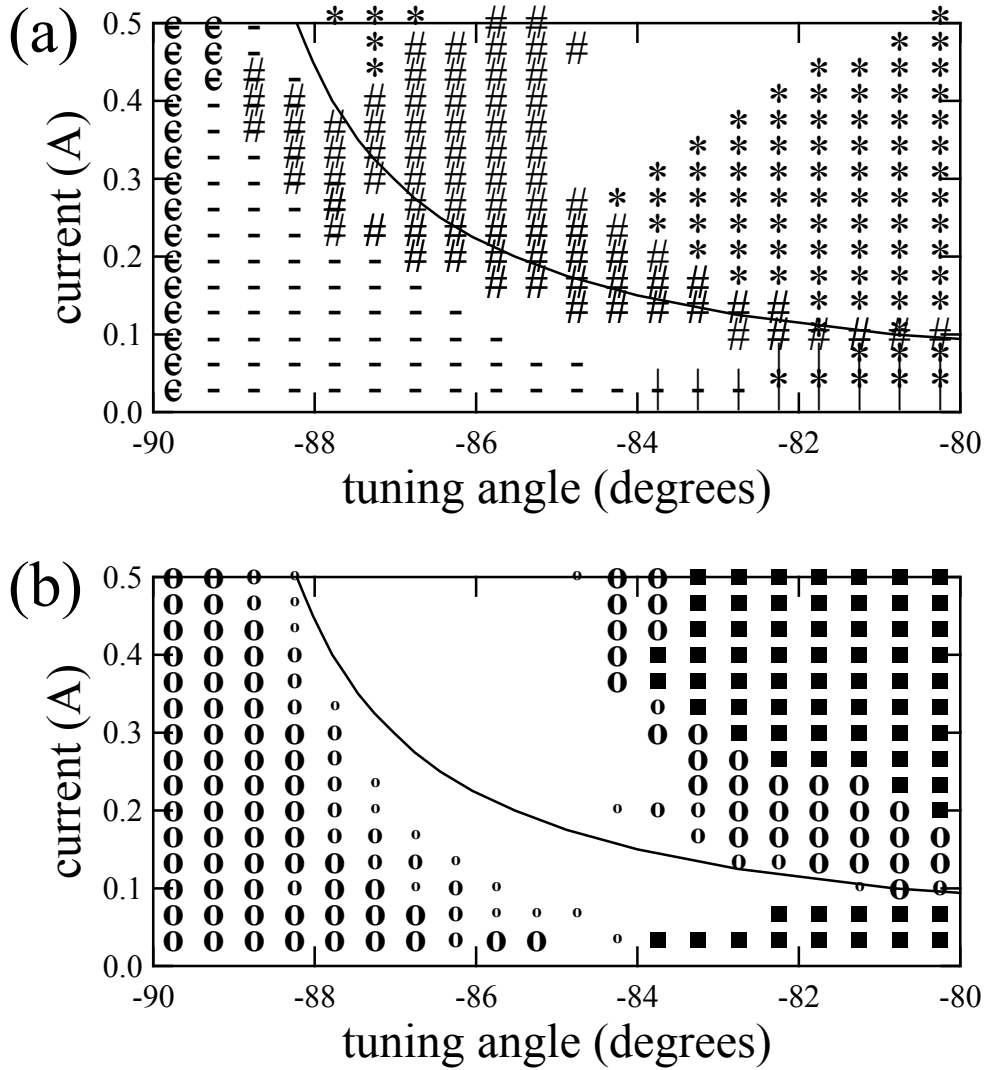


Figure 2. Instability modeling for passive harmonic-cavity operation at HLSII, in which worst-case parasitic coupled bunch instability is considered. (a) Analytic instability predictions. -: parasitic coupled bunch instability, |: coupled dipole Robinson instability; *: coupled quadrupole Robinson instability; #: fast mode-coupling Robinson instability; c: coupled-bunch instability with longitudinal mode number of 1. (b) Results of 500,000-turn simulations of 4500 macroparticles. o : mild instability, where the energy spread exceeds its natural value by 10–30%; o: moderate instability, where the energy spread has increased by 30–100%; O: strong instability, where the energy spread has increased more than 100%; ■: lost macroparticles.

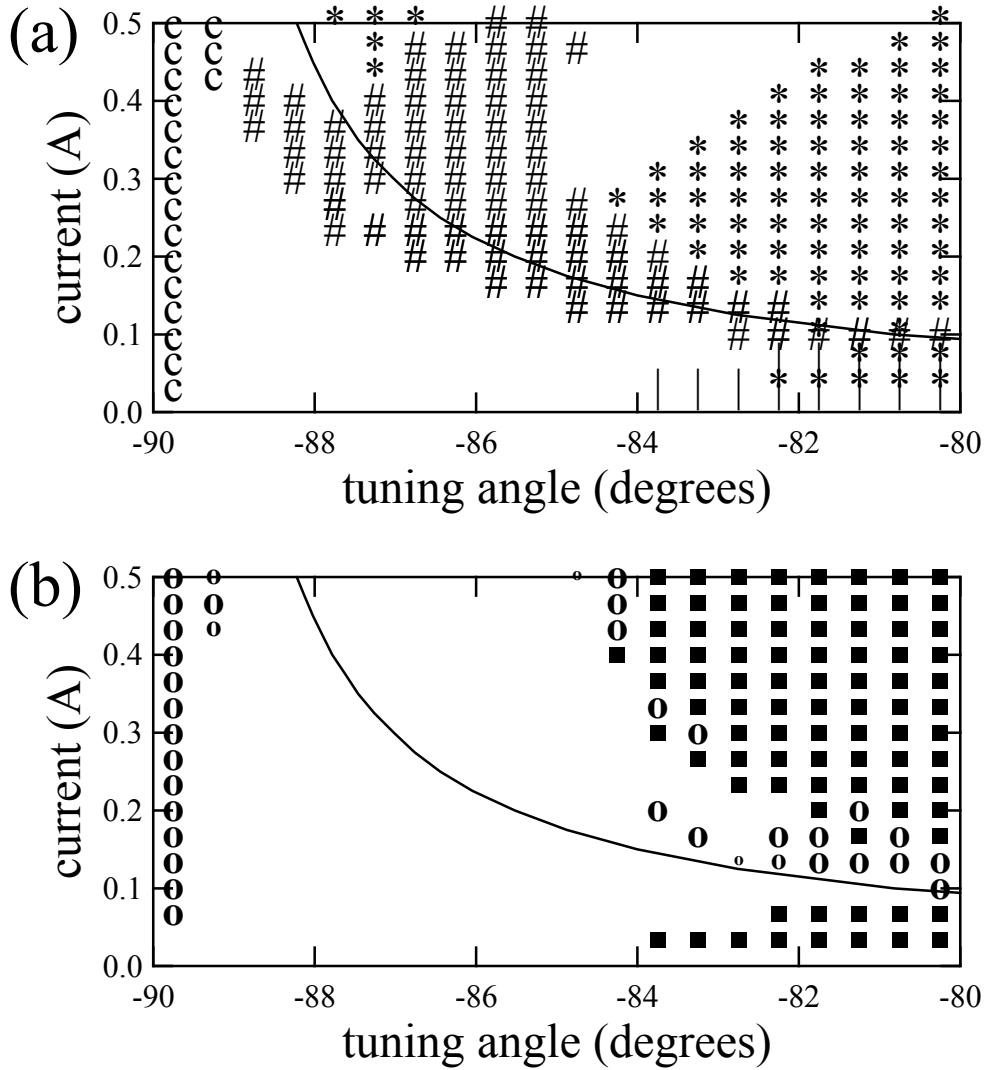


Figure 3. Instability modeling for passive harmonic-cavity operation at HLSII with an HOM representing a broadband impedance $|Z_p / p| = 0.125 \Omega$. (a) Analytic instability predictions. m: microwave instability, |: coupled dipole Robinson instability; *: coupled quadrupole Robinson instability; #: fast mode-coupling Robinson instability; c: coupled-bunch instability with longitudinal mode number of 1. (b) Results of 500,000-turn simulations of 180,000 macroparticles. o: mild instability, where the energy spread exceeds its natural value by 10–30%; o: moderate instability, where the energy spread has increased by 30–100%; O: strong instability, where the energy spread has increased more than 100%; ■: lost macroparticles.

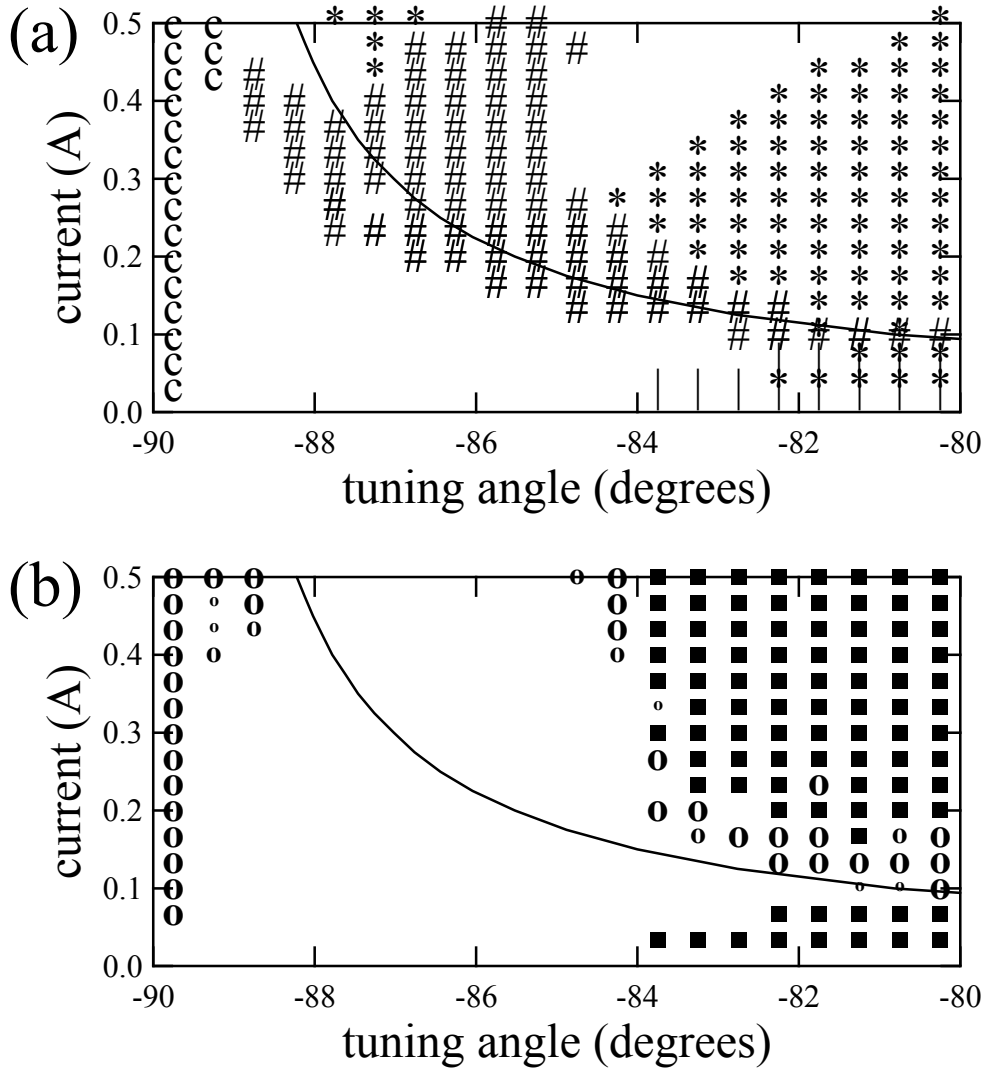


Figure 4. Instability modeling for passive harmonic-cavity operation at HLSII with an HOM representing a broadband impedance $|Z_p / p| = 0.25 \Omega$. (a) Analytic instability predictions. m: microwave instability, |: coupled dipole Robinson instability; *: coupled quadrupole Robinson instability; #: fast mode-coupling Robinson instability; c: coupled-bunch instability with longitudinal mode number of 1. (b) Results of 500,000-turn simulations of 180,000 macroparticles. o: mild instability, where the energy spread exceeds its natural value by 10–30%; o: moderate instability, where the energy spread has increased by 30–100%; O: strong instability, where the energy spread has increased more than 100%; ■: lost macroparticles.

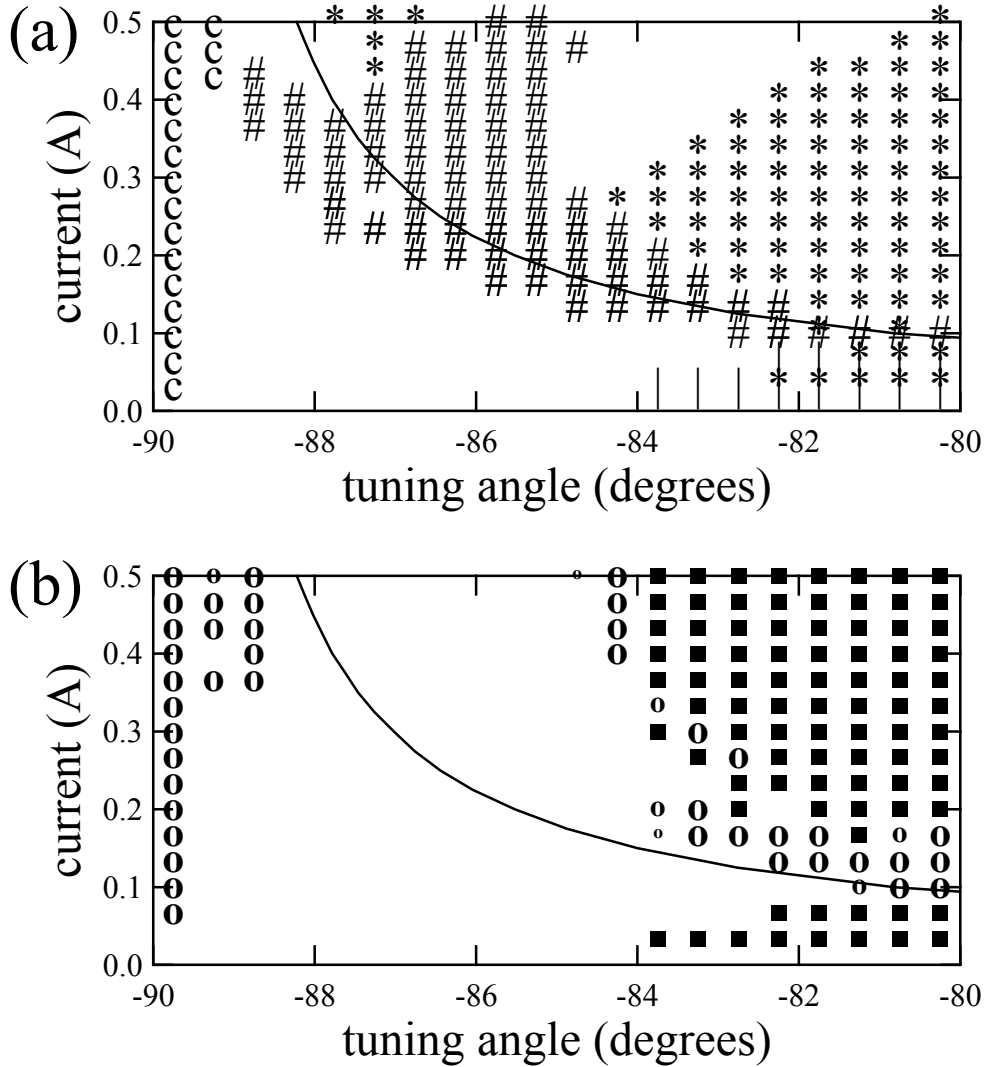


Figure 5. Instability modeling for passive harmonic-cavity operation at HLSII with an HOM representing a broadband impedance $|Z_p/p| = 0.5 \Omega$. (a) Analytic instability predictions. m: microwave instability, |: coupled dipole Robinson instability; *: coupled quadrupole Robinson instability; #: fast mode-coupling Robinson instability; c: coupled-bunch instability with longitudinal mode number of 1. (b) Results of 500,000-turn simulations of 180,000 macroparticles. o: mild instability, where the energy spread exceeds its natural value by 10–30%; o: moderate instability, where the energy spread has increased by 30–100%; o: strong instability, where the energy spread has increased more than 100%; ■: lost macroparticles.

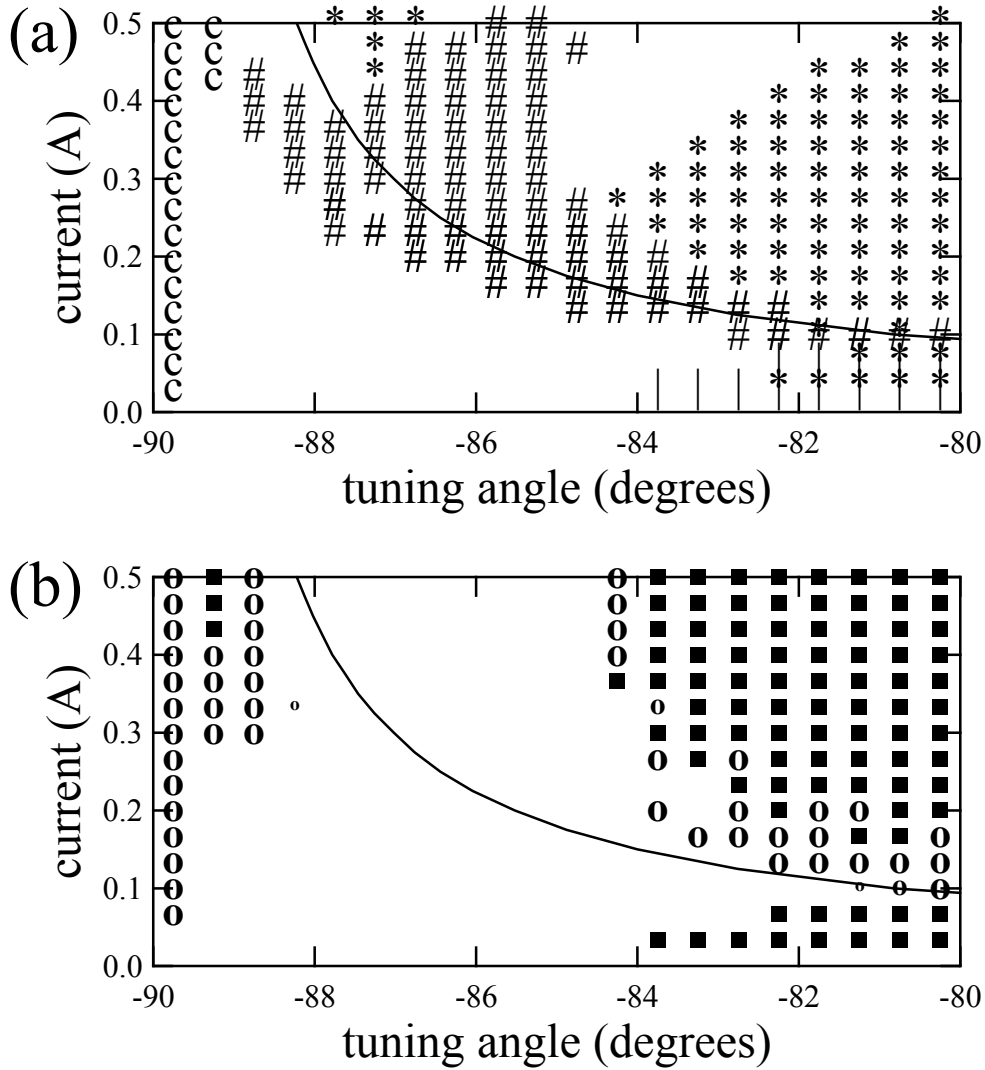


Figure 6. Instability modeling for passive harmonic-cavity operation at HLSII with an HOM representing a broadband impedance $|Z_p/p|=1\Omega$. (a) Analytic instability predictions. m: microwave instability, |: coupled dipole Robinson instability; *: coupled quadrupole Robinson instability; #: fast mode-coupling Robinson instability; c: coupled-bunch instability with longitudinal mode number of 1. (b) Results of 500,000-turn simulations of 180,000 macroparticles. o: mild instability, where the energy spread exceeds its natural value by 10–30%; ●: moderate instability, where the energy spread has increased by 30–100%; ○: strong instability, where the energy spread has increased more than 100%; ■: lost macroparticles.

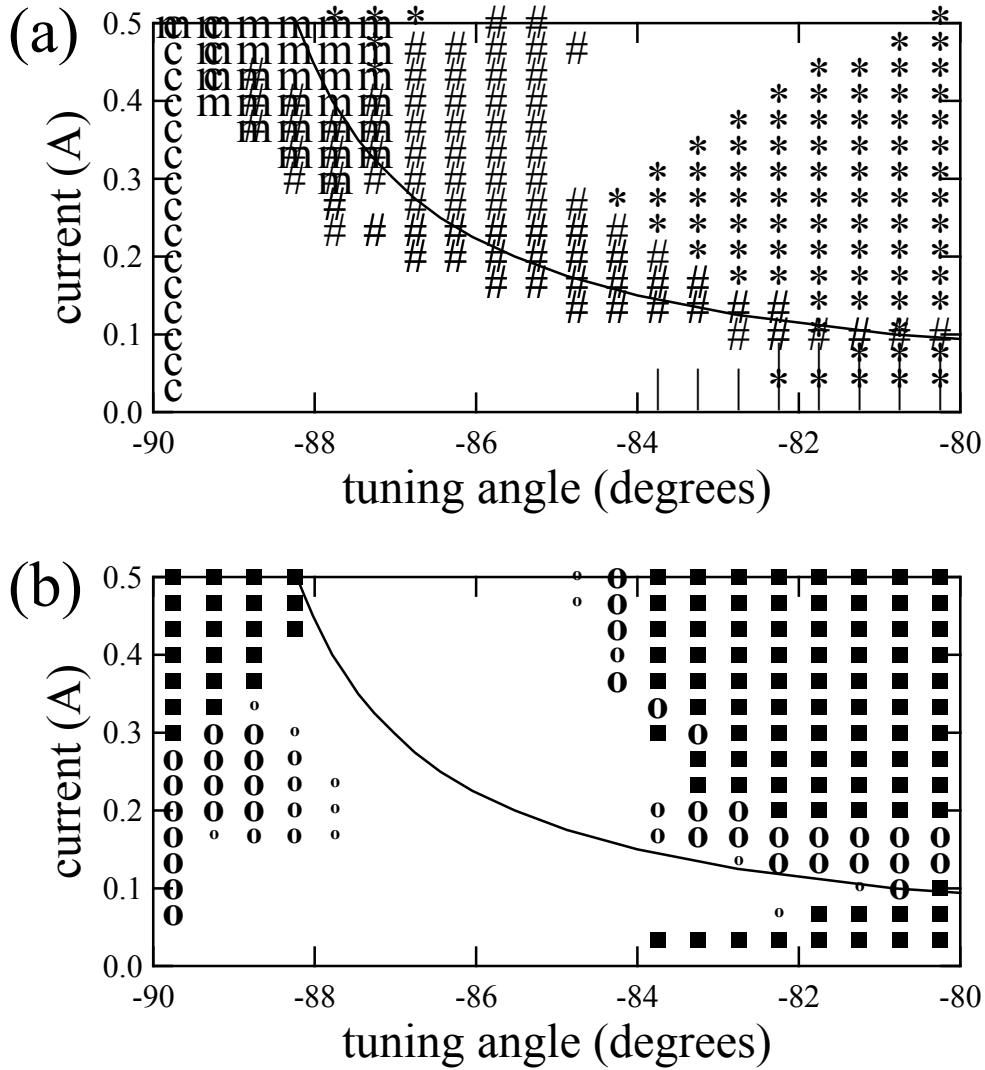


Figure 8. Instability modeling for passive harmonic-cavity operation at HLSII with an HOM representing a broadband impedance $|Z_p/p| = 4 \Omega$. (a) Analytic instability predictions. m: microwave instability, |: coupled dipole Robinson instability; *: coupled quadrupole Robinson instability; #: fast mode-coupling Robinson instability; c: coupled-bunch instability with longitudinal mode number of 1. (b) Results of 500,000-turn simulations of 180,000 macroparticles. o: mild instability, where the energy spread exceeds its natural value by 10–30%; o: moderate instability, where the energy spread has increased by 30–100%; O: strong instability, where the energy spread has increased more than 100%; ■: lost macroparticles.

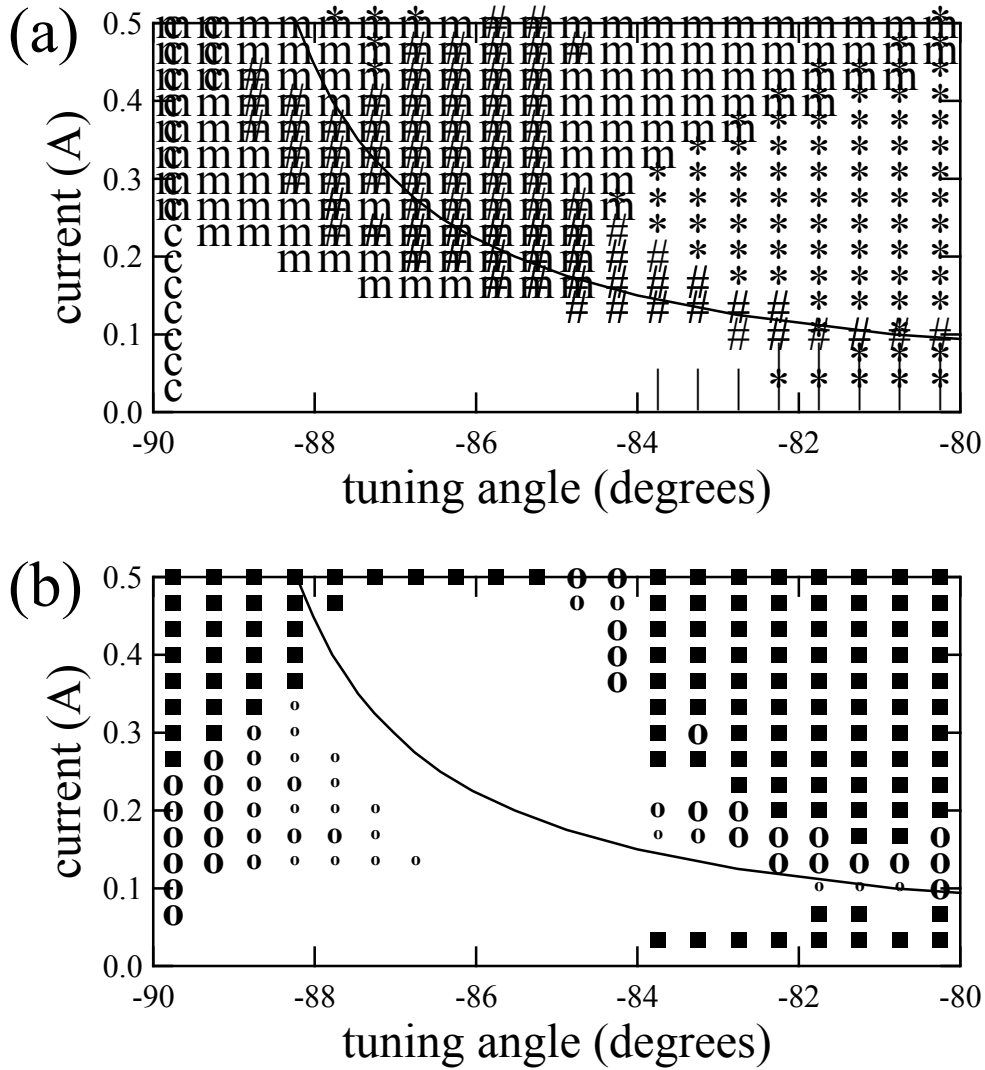


Figure 9. Instability modeling for passive harmonic-cavity operation at HLSII with an HOM representing a broadband impedance $|Z_p/p| = 8 \Omega$. (a) Analytic instability predictions. m: microwave instability, |: coupled dipole Robinson instability; *: coupled quadrupole Robinson instability; #: fast mode-coupling Robinson instability; c: coupled-bunch instability with longitudinal mode number of 1. (b) Results of 500,000-turn simulations of 180,000 macroparticles. o: mild instability, where the energy spread exceeds its natural value by 10–30%; o: moderate instability, where the energy spread has increased by 30–100%; O: strong instability, where the energy spread has increased more than 100%; ■: lost macroparticles.

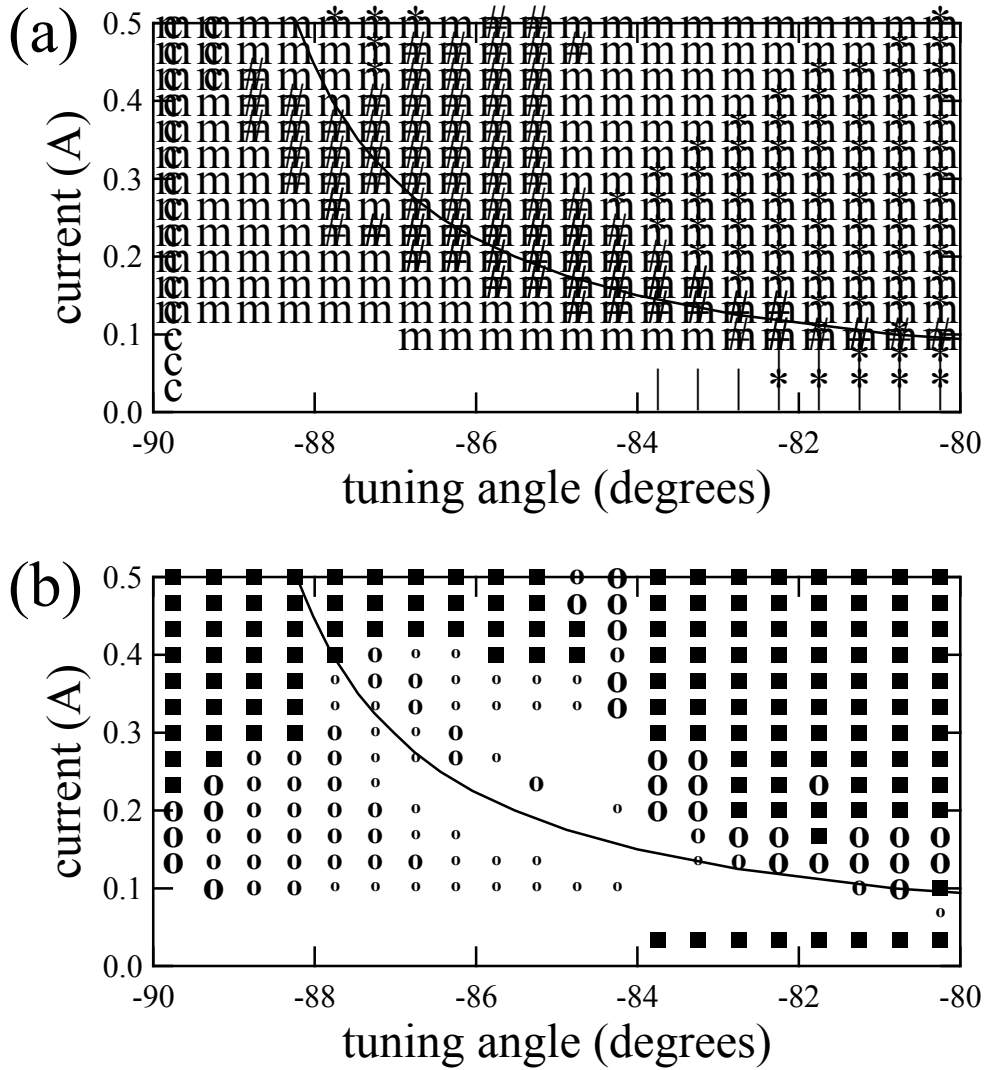


Figure 10. Instability modeling for passive harmonic-cavity operation at HLSII with an HOM representing a broadband impedance $|Z_p / p| = 16 \Omega$. (a) Analytic instability predictions. m: microwave instability, |: coupled dipole Robinson instability; *: coupled quadrupole Robinson instability; #: fast mode-coupling Robinson instability; c: coupled-bunch instability with longitudinal mode number of 1. (b) Results of 500,000-turn simulations of 180,000 macroparticles. o: mild instability, where the energy spread exceeds its natural value by 10–30%; o: moderate instability, where the energy spread has increased by 30–100%; O: strong instability, where the energy spread has increased more than 100%; ■: lost macroparticles.

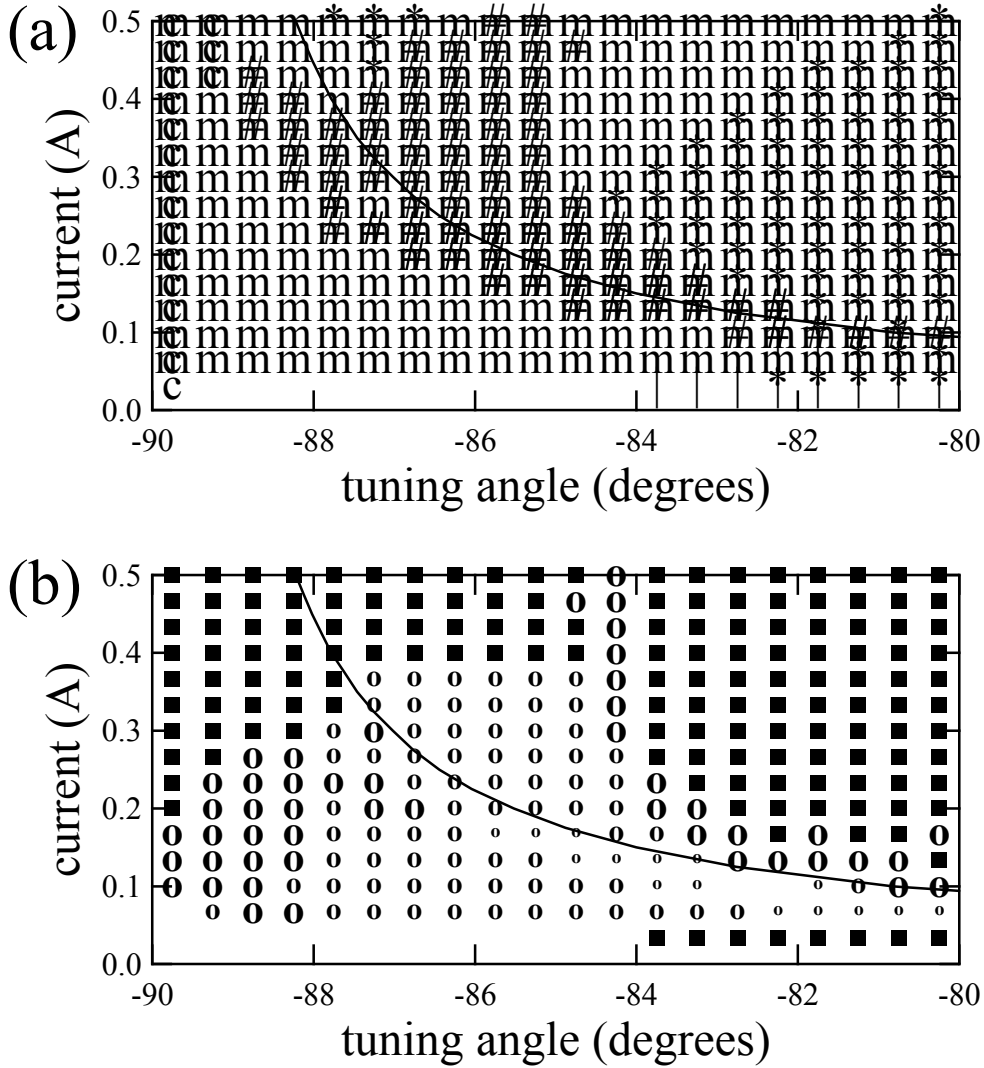


Figure 11. Instability modeling of passive harmonic-cavity operation at HLSII with an HOM representing a broadband impedance $|Z_p / p| = 32 \Omega$. (a) Analytic instability predictions. m: microwave instability, |: coupled dipole Robinson instability; *: coupled quadrupole Robinson instability; #: fast mode-coupling Robinson instability; c: coupled-bunch instability with longitudinal mode number of 1. (b) Results of 500,000-turn simulations of 180,000 macroparticles. o: mild instability, where the energy spread exceeds its natural value by 10–30%; o: moderate instability, where the energy spread has increased by 30–100%; O: strong instability, where the energy spread has increased more than 100%; ■: lost macroparticles.